# A Neural Network Approach to Control Allocation of Ships for Dynamic Positioning

Robert Skulstad*[1], Guoyuan Li[1], Houxiang Zhang[1], and Thor I. Fossen[2]

[1]Norwegian University of Science and Technology, Department of Ocean Operations and Civil Engineering, Aalesund, Norway (e-mail: robert.skulstad, guoyuan.li, hozh @ntnu.no).
[2]Norwegian University of Science and Technology, Department of Engineering Cybernetics, Trondheim, Norway (e-mail: thor.fossen@ntnu.no).

**Abstract**

Dynamic Positioning (DP) of ships is a control mode that seeks to maintain a specific position (stationkeeping) or perform low-speed maneuvers. In this paper, a static Neural Network (NN) is proposed for control allocation of an over-actuated ship. The thruster force and commands are measured during a trial run of the simulated vessel to gather data for training of the NN. Then the network is trained and used to transform the virtual force commands from a motion controller into individual thruster commands. A standard Proportional Integral Derivative (PID) controller, using wave-filtered position and heading measurements, is implemented as motion controller for each Degree Of Freedom (DOF) of the ship. For a DP application the controllable DOFs are the translational motion in surge and sway directions, as well as the rotation about its up/down axis. Simulation tests were performed to verify the feasibility of this approach.

***Keywords***— PID controllers, Neural-network models, Dynamic positioning, Control allocation

## 1 Introduction

Ships that are involved in safety-critical operations related to drilling, cargo-transfer, subsea crane operations and pipe-laying typically have an extended actuator setup to allow for redundancy in case of system errors. During such operations the vessel is required to control its position and heading. This operational mode is known as Dynamic Positioning (DP), which performs stationkeeping or low-speed maneuvering. In terms of the degrees of freedom (DOF) of the vessel, DP normally controls the surge (longitudinal), sway (lateral) and yaw (rotation about the up/down axis) simultaneously. Conventional ships use either tunnel thrusters, azimuth thrusters or main thrusters for thrust generation

In order to perform DP operations a modular approach to motion control is often applied (Johansen and Fossen (2013)). A top-level motion controller converts the error between the desired state and the actual state of the ship, into a generalized force vector in surge/sway direction and moment about the yaw axis. Then a control allocation module distributes that force vector into individual thruster commands to fulfill the requirements of the motion controller.

Historically, optimization-based control allocation techniques have dominated. This allows for flexibility in terms of optimization goal (and sub-goals), motivating advances in minimum power schemes and minimization of actuator wear. Lindegaard and Fossen (2003) exploited the operation of a rudder for lateral thrust to derive an energy-efficient thrust allocation algorithm for low speed operations. An explicit two-step solution was suggested to calculate a feasible thrust vector, u. The approach was limited to one rudder at a time. Their algorithm was extended by Johansen et al. (2008) to allow any number of rudders. Magnitude and rate constraints were also accounted for. Perez and Donaire (2009) handled both magnitude constraints and rate constraints in the top-level motion controller by an anti-windup controller. By constraining the virtual control vector from the motion controller, they could perform unconstrained control allocation which was posed as an optimization problem. The solution to this unconstrained control allocation may be found in (Fossen (2011)).

*Corresponding author

Sørdalen (1997) used filtering techniques to tackle the problem of azimuth angle rate constraints for rotatable thrusters. Without this constraint consideration, a singular thruster configuration may occur when rotatable thrusters are used actively. The result is failing to meet the control commands of the control law.

An adaptive genetic algorithm was used to solve the thrust allocation problem in (Zhao et al. (2010)). A fitness function was constructed based on an objective function with constraints. They considered thrust allocation for a semi-submersible rig using rotatable thrusters. Constraints considered were thruster force limits, its change rate, angular rate of thrusters and respective forbidden azimuth angles. Bui and Kim (2011) presented a control allocation scheme that involved the use of external thrust providers in the form of autonomous tugboats for ship berthing application. A constrained optimization problem was used, which they solved using a redistributed pseudo-inverse algorithm.

Chen and Jiang (2012) transformed the constrained allocation task into a convex quadratic programming problem for constrained control allocation. To solve this they applied a recurrent neural network. A neural network control algorithm was applied in (Zhang et al. (2017)) to overcome actuator gain uncertainties and to compensate for unmodelled environmental disturbances. The algorithm was tested in a simulator using six thrusters, where one of them was rotatable. Realistic environmental disturbances were applied in the simulation test.

Except for the approach described by Zhang et al. (2017), the methods described above require knowledge about the command-to-force relationship of each thruster.

Within the aerospace industry, control allocation has also received significant attention. An overview of methods used within this domain is given in Oppenheimer et al. (2006), while an evaluation of methods is given in Bodson (2002).

In this article we propose to use a neural network to obtain the mapping between the virtual generalized force, commanded by the motion controller, and the individual thruster commands. It will consider thruster rate constraints as well as limiting the maximum and minimum commands of the thrusters (magnitude constraint) for non-rotatable thrusters. Manual operation of the thrusters is used to generate the training data. Sequentially, each thruster was put through its entire operational range by first ordering a maximum command. Then, when maximum was reached, a minimum command was issued. In addition to reaching maximum/minimum thruster command values, this commands the maximum change rate as well. In this paper, no explicit support for relative weighting between thrusters exist. To achieve this, the designer would have to supply the network with a training set that reflected the desired weighting. This could be a restricted operational range for the main thrusters, resulting in lower force output by those thrusters. Two assumptions were made:

- The forces and moments imparted by each thruster on the vessel are measurable.
- The command-to-force relation gathered in the test set for calm seas is representative for command-to-force relations in all other sea states.

To validate the scheme, and for collecting training data for the NN allocation mapping, a simulated vessel will be used.

# 2 Control scheme

As noted by Johansen and Fossen (2013) there typically exists a hierarchy in the control system for over-actuated mechanical systems. This hierarchy allows for a modular design where each module is self-contained. Figure 1 gives an overview of the complete system used in this paper. $\tau_c$ is the commanded virtual force and moment given in the vessel frame of reference. $u$ is the vector of individual control commands. $\tau$ is the individual horizontal plane forces imparted on the virtual ship by the thrusters. $\tau_{env}$ are the forces acting on the vessel through environmental disturbances. Included in the PID Motion controller module (section 2.2) is a wave filter, which will be described in section 2.1. The NN control allocation module of figure 1 contains both an initial training algorithm and a forward calculation of the control vector $u$. The latter operation is executed at each step of the complete system. An update rate of 20 Hz was used. The output of the control allocation module will be input directly to each thruster.

## 2.1 Wave filter

Prior to sending the relevant measurements to a control system it is customary to filter the signals to avoid compensating for high-frequency wave-induced motion (Fossen and Perez (2009)). This process is

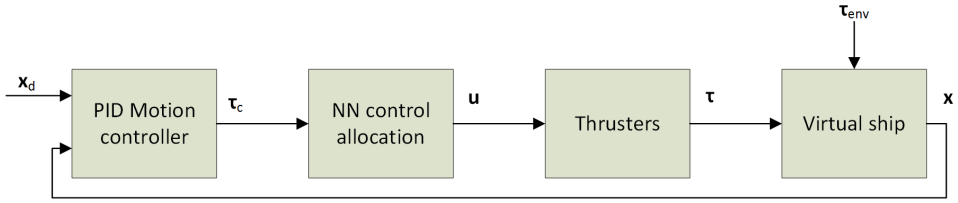


Figure 1: Overview of the proposed scheme for DP using NN allocation.

therefore often referred to as wave-filtering and is a necessary step to reduce wear and tear on actuators. Several tools can be used for this purpose including low-pass filters, Kalman filters and observers (Fossen (2011)). Low-pass filters are utilized in this stage. Although it has limited effect due to the phase lag incurred, they do not require prior knowledge of either vessel dynamics or the impact of environmental forces on the vessel.

## 2.2 PID motion controller

A standard PID controller was used to obtain the virtual forces necessary to converge to a given desired state. The need for integral action is evident when considering the drift force exerted on the vessel by wind, low frequency wave drift forces and ocean currents. Position measurements were given in the local North East Down (NED) frame. This made it necessary to rotate the position in the horizontal plane in order to provide error metrics aligned with the coordinate frame of the vessel. For DP operation, we define the state vector in the NED reference frame as $[N, E, \psi]^T$ and $[X, Y, \psi]^T$ for the state vector in the vessel reference frame. $\psi_d$ is the desired heading angle of the vessel. Figure 2 shows the X and Y axis of the vessel-bound state vector.

Equation 1 yields the error signal which will act as input to the PID motion controller.

$$\begin{bmatrix} X_{err} \\ Y_{err} \\ \psi_{err} \end{bmatrix} = \boldsymbol{R}^{-1}(\psi) \left( \begin{bmatrix} N_d \\ E_d \\ \psi_d \end{bmatrix} - \begin{bmatrix} N \\ E \\ \psi \end{bmatrix} \right) \tag{1}$$

Obtaining the virtual control vector is achieved by applying a PID controller for each DOF represented in the vessel fixed state vector.

$$\tau_c = \begin{bmatrix} F_X \\ F_Y \\ M_\psi \end{bmatrix} = \begin{bmatrix} PID(X_{err}) \\ PID(Y_{err}) \\ PID(\psi_{err}) \end{bmatrix} \tag{2}$$

where $PID(e) = K_p * (e + 1/T_i * \int_0^t e + T_d * \dot{e})$ and $K_p$, $T_i$ and $T_d$ are parameters of the PID regulator subject to tuning for desired response. $F_X$ is the surge force, $F_Y$ is the sway force and $M_\psi$ is the yaw moment required by the motion controller.

## 2.3 Neural network control allocation

A NN was used to provide the transformation between desired generalized forces (input) and the individual thruster commands (output). More specifically the learning methodology adopted was that of the Extreme Learning Machine (ELM) introduced by Guang-Bin Huang et al. (2004). Two main approaches exist with regards to adapting structure and weight parameters of the network. The most basic one involves a single, initial, calculation of weights, either using a fixed structure or adapting the structure by means of pruning/constructive methods. Alternatively, one may update both structure and weights iteratively, termed online learning, to adapt the network to time-varying properties of the process which produces the data. In this paper we adopt the first approach, fixing the structure and the weights of the network initially. Furthermore, the ELM is capable of approximating any continuous target function given proper architecture and sufficient training data. This, along with the efficiency of the algorithm, motivated the choice of using a shallow network structure as opposed to a deep neural network. The learning process of the ELM is outlined below using the same notation as Huang et al. (2011).

$$\mathbf{H} = \begin{bmatrix} \mathbf{G}(\mathbf{a}_1, b_1, \mathbf{x}_1) & \dots & \mathbf{G}(\mathbf{a}_L, b_L, \mathbf{x}_1) \\ \vdots & \dots & \vdots \\ \mathbf{G}(\mathbf{a}_1, b_1, \mathbf{x}_N) & \dots & \mathbf{G}(\mathbf{a}_L, b_L, \mathbf{x}_N) \end{bmatrix} \tag{3}$$

**H** is a N-by-L matrix, where N represents the number of input vectors available and L is the number of hidden layer neurons. Each node in the middle/hidden layer applies the activation function $\mathbf{G}(\mathbf{a}, b, \mathbf{x})$, where **a** is a vector of incoming weights, b is a random bias value and **x** is the input vector. A sigmoid activation function was applied for each hidden layer neuron. The only remaining unknown is the output layer weight matrix $\boldsymbol{\beta}$. This is determined using the Moore-Penrose generalized inverse as shown in equation 4. The learning scheme falls under the category of supervised learning and $\boldsymbol{T}$ therefore signifies the known true output of the system given an input vector.

$$\boldsymbol{\beta} = \boldsymbol{H}^{\dagger}\boldsymbol{T} \tag{4}$$

The condensed stepwise algorithm is given below for readability.

1. Assign random numbers to the input-to-hidden layer weights
2. Calculate the hidden layer output matrix according to equation 3
3. Determine the output layer weight parameters according to equation 4

We define two variations of the control allocation unit for comparison of performance. They differ only in terms of the structure of the NN allocator:

- Allocator 1: Only the generalized forces were applied as input to the network.
- Allocator 2: The input thrust command is augmented using the applied commands from the previous time step.

#### 2.3.1 Allocator 1

As mentioned, the implementation of Allocator 1 used only the generalized force/moment vector issued from the motion controller as input. This is the common interface signal used by the methods referenced in the introduction. The output was the five individual command signals. To determine the proper hidden layer neuron number several different neuron numbers were tested. The neuron number corresponding to the lowest Root Mean Square Error (RMSE), based on validation by randomly selected input/target pairs of the entire training set, was selected. This approach yielded a NN structure of 3 input neurons, 20 hidden layer neurons and 6 output neurons. This mapping remained fixed for the duration of the test case given in section 3.2.

#### 2.3.2 Allocator 2

As a means to add additional information about the rate changes experienced in the training set the input to the allocation unit was augmented. The new input consisted of the same generalized forces as in Allocator 1, in addition to the commands issued to each thruster at the previous time step. Otherwise the two allocation implementations (1 and 2) were identical. For both allocators a training set of 7800 samples was used.

## 3 Simulation results

Simulations were carried out in a commercial marine vessel simulator developed by the Norwegian company Offshore Simulator Centre (OSC) AS. Test case parameters are given in section 3.1.

### 3.1 Test case description

The vessel, shown in figure 2, was ordered to remain fixed at a position of (0,0) m in the NED reference frame and a heading angle of 0 degrees. To achieve this the vessel utilized 6 thrusters. The two stern-mounted main thrusters, which were operated in tandem, required a command of blade pitch angle (thrusters marked 5 and 6 in figure 2). Two sets of individually operated tunnel thrusters were located at the bow and stern of the vessel (thrusters marked 1-4 in figure 2). Both set of thrusters were operated using RPM commands. All thrusters were considered non-rotatable, producing positive thrust in the direction of the arrow accompanying each thruster in figure 2. Considering that the vessel is controlled in three DOFs and the number of individually operated thrusters are 5, the vessel is over-actuated. External disturbances were applied at a fixed direction, from north to south. Initially a uniform wind

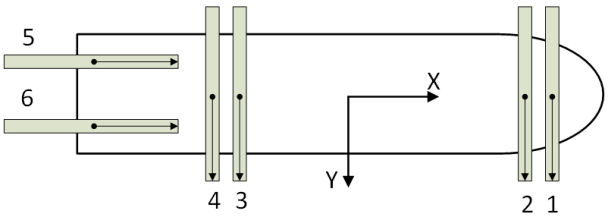


Figure 2: The vessel and its thruster layout. Note that the two leftmost thrusters (main thrusters) supply thrust in the positive/negative x-direction only.

velocity of 4 m/s affects the vessel. At the start of figure 3, a step change in wind is applied with a final value of 8 m/s. Waves generated using the JONSWAP spectrum, were applied. Both first and second order wave forces affected the vessel in the same direction as the wind and with a significant wave height of 2 meters.

In order to initialize the control allocation mapping described in section 2.3, a test set of previously recorded simulation data was used. Commanded thruster setpoint, actual thrust in Newton and the torque in Newton meter imparted by each thruster on the vessel, were recorded for the purpose of training the neural network. Each thruster was operated to its maximum and minimum command value, thus exposing its complete operational range. The model of the virtual vessel is derived from a real vessel and thus its thrusters have specific constraints with regards to command magnitude and change rate. Table 1 shows the thruster constraints.

Table 1: Specification of thruster operational constraints.

| Thruster | Max | Min | Rate change |
|---|---|---|---|
| 1,2 | 204.00 RPM | -204.00 RPM | 20.40 RPM/s |
| 3,4 | 276.00 RPM | -276.00 RPM | 27.60 RPM/s |
| 5,6 | 28.70 deg | -21.50 deg | 1.44 deg/s |

Although the motion controller is not the main focus of this paper, a reasonable performance is still required to provide sensible input data to the allocation unit. For this purpose a standard PID controller was applied to each of the DOFs of the vessel. To reduce the adverse effects of high frequency wave-induced motion a low-pass filter was applied to the input signals in the motion controller shown in figure 1. This was done prior to calculating the generalized forces.

## 3.2 Allocator 1

Figure 3 shows the performance of the complete system, which is to remain at a fixed location and heading. The red lines of figure 3 describe the performance of the system using allocator 1. The rapid change rate of this allocator allows it to compensate for the step change quickly and therefore minimize the deviation from the desired desired position. However, the red line of the middle plot of figure 3 reveals slow convergence in the East direction. The high-frequency overloaded signal seen in all plots in figure 3 is caused by the vessel interacting with waves.

Figure 4 shows the output from the allocation unit for allocator 1. It is evident that the commands generated by the allocation unit is very sensitive to variation in the generalized force command. This might suggest that further wave-filtering and controller tuning might be required for this implementation to be useful. The excessive changes in thruster commands are also visible in figure 5, showing the change in command between time steps and also the maximum change allowed for each thruster. The sampling frequency of the system was set to 20 Hz, yielding the rate limit in figures 5 and 7 based on table 1

## 3.3 Allocator 2

Allocator 2 is less aggressive relative to allocator 1, although the same parameters for the PID regulators have been used. The derived thruster commands change more slowly, yielding increased settling times. Similar to allocator 1, the East direction (middle plot of figure 3) response shows the slowest convergence.

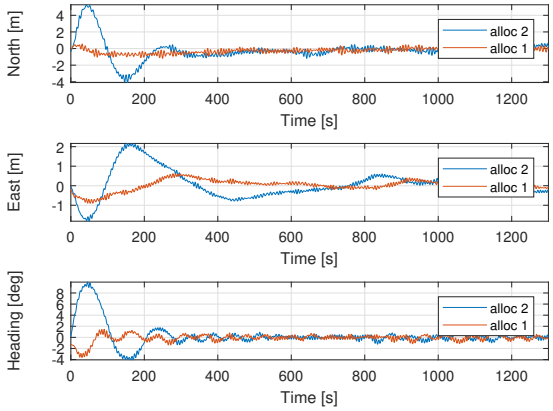


Figure 3: The position and heading of the vessel recorded during the test case run for both allocator 1 and 2.

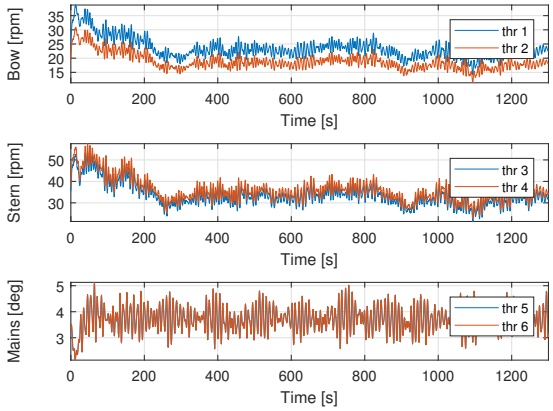


Figure 4: The commands input to each of the thrusters for the test case using allocator 1. Top: RPM commands issued to the bow tunnel thrusters. Middle: RPM commands to the stern tunnel thrusters. Bottom: Blade pitch angle commands issued to the two aft main thrusters.

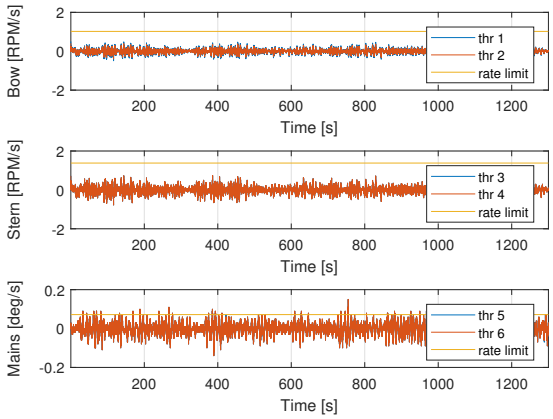


Figure 5: Shows the change rate of the commands issued to each thruster.

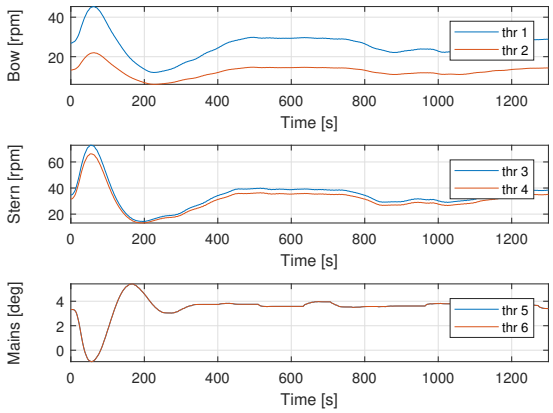


Figure 6: The commands input to each of the thrusters for the test case using allocator 2. Top: RPM commands issued to the bow tunnel thrusters. Middle: RPM commands to the stern tunnel thrusters. Bottom: Blade pitch angle commands issued to the two aft main thrusters.

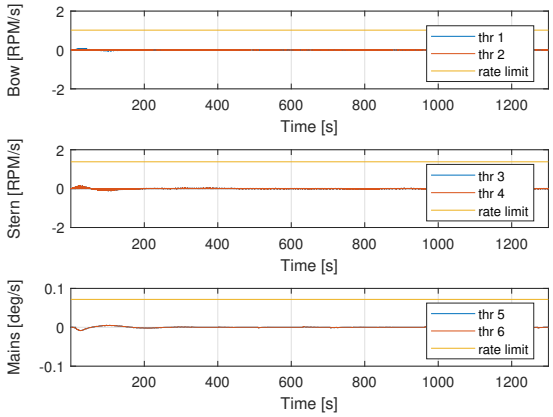


Figure 7: Shows the change rate of the commands issued to each thruster.

The commands issued by this allocator implementation result in a significant reduction in command rate of change.

Figure 7 shows the reduction in rate change due to the augmented input vector of Allocator 2. Rate constraints for all thrusters were satisfied using this implementation.

## 3.4 Magnitude constraint

More severe external disturbances were necessary to approach the maximum thrust limits for the thrusters. The wind and wave direction was set to act from west to east while the vessel attempted to maintain zero heading and position. Significant wave height was increased to 3 meters and the wind velocity was set to increase from 4 m/s to 20 m/s. This wind velocity increase took place at t = 2500 seconds. The result of increasing the lateral force imparted on the vessel is given in figure 8.

Figure 9 gives the corresponding thruster setpoint commands issued from the allocation unit. For this specific test Allocator 2 was used. The figure shows that the commands for thrusters 1-4 saturates, rendering the vessel under-powered in the lateral direction. Insufficient thrust force causes the vessel to drift off in the east direction (see the middle plot of figure 8) as well as failing to converge to a zero heading angle.

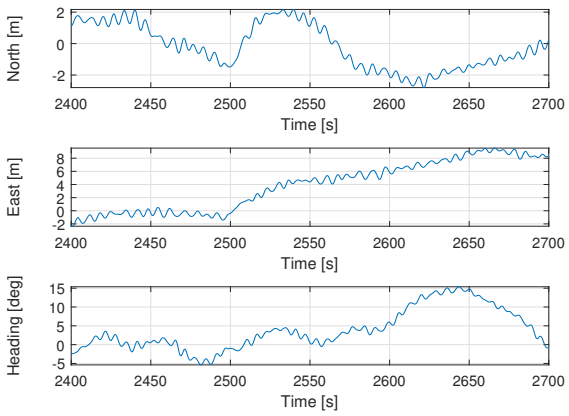


Figure 8: Recorded position and heading during the magnitude constraint test.

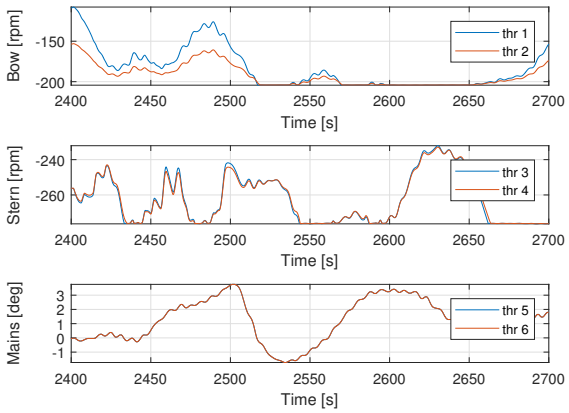


Figure 9: Displays the thruster setpoint commands for all thrusters. Top and middle plot shows saturation due to the environmental disturbances impacting the port side of the vessel.

# 4 Discussion

With an augmented input vector, the control allocation NN has been shown to provide constraint handling for rate change and magnitude of thrusters on a simulated vessel. Allocator 2 displays the most realistic implementation, adhering to the rate constraints present in the dataset used for training. It is therefore necessary to provide a training set that reflects the constraints of the vessel, meaning that to achieve the maximum rate change the thrusters on the vessel must be operated at its maximum rate when logging the training data. The use of thrust force measurements limits the applicability of this approach to simulators.

The test constructed to verify the ability of the NN allocator to deal with thruster magnitude constraints may not represent conditions that will be faced by a real vessel. However, it pushes the NN allocation to its thresholds, showing that it is able to constrain the commands based on the dataset used for training the NN.

Although not verified in this paper, thruster failure scenarios may be handled by a re-training step of the NN allocation mapping. For the training set and NN architecture used in this paper, the entire re-training procedure is performed in 1.3 seconds. More sophisticated functionality such as power minimization, support for thrusters rotatable in the range $[-180, 180 >$ degrees and support for forbidden zones of rotatable thrusters were not considered. They will be the aim for future improvements of the suggested approach.

# 5 Conclusion

In this paper we introduce a neural network thruster allocation scheme that only relies on thruster force and command measurements. Though systems onboard real vessels do not accomodate thrust force measurements, we seek here to promote an approach to control allocation that does not rely on knowledge about the specific thruster parameters. The augmented version of the neural network allocator is able to learn the relationship between the generalized thrust and thruster commands as well as handling maximum/minimum and rate constraints.

# 6 Acknowledgement

The authors would like to thank OSC for their support in relation to performing the simulation study.

# References

Bodson, M. (2002). Evaluation of Optimization Methods for Control Allocation. *Journal of Guidance, Control, and Dynamics*, 25(4):703–711.

Bui, V. P. and Kim, Y. B. (2011). Development of constrained control allocation for ship berthing by using autonomous tugboats. *International Journal of Control, Automation and Systems*, 9(6):1203–1208.

Chen, M. and Jiang, B. (2012). Adaptive control and constrained control allocation for overactuated ocean surface vessels. *International Journal of Systems Science*, 7721(November):1–15.

Fossen, T. I. (2011). *Handbook of Marine Craft Hydrodynamics and Motion Control*. John Wiley & Sons Ltd.

Fossen, T. I. and Perez, T. (2009). Kalman Filtering for Positioning and Heading Control of Ships and Offshore Rigs: Estimating the effects of waves, wind, and current. *IEEE Control Systems*, 29(6):32–46.

Guang-Bin Huang, Qin-Yu Zhu, and Chee-Kheong Siew (2004). Extreme learning machine: a new learning scheme of feedforward neural networks. In *2004 IEEE International Joint Conference on Neural Networks*, pages 985–990.

Huang, G. B., Wang, D. H., and Lan, Y. (2011). Extreme learning machines: A survey. *International Journal of Machine Learning and Cybernetics*, 2(2):107–122.

Johansen, T. A. and Fossen, T. I. (2013). Control allocation - A survey. *Automatica*, 49(5):1087–1103.

Johansen, T. A., Fuglseth, T. P., Tøndel, P., and Fossen, T. I. (2008). Optimal constrained control allocation in marine surface vessels with rudders. *Control Engineering Practice*, 16(4):457–464.

Lindegaard, K. P. and Fossen, T. I. (2003). Fuel-efficient rudder and propeller control allocation for marine craft: Experiments with a model ship. *IEEE Transactions on Control Systems Technology*, 11(6):850–862.

Oppenheimer, M. W., Doman, D. B., and Bolender, M. A. (2006). Control allocation for over-actuated systems. In *14th Mediterranean Conference on Control and Automation, MED'06*, number 2.

Perez, T. and Donaire, A. (2009). Constrained control design for dynamic positioning of marine vehicles with control allocation. *Modeling, Identification and Control*, 30(2):57–70.

Sørdalen, O. J. (1997). Optimal thrust allocation for marine vessels. *Control Engineering Practice*, 5(9):1223–1231.

Zhang, G., Cai, Y., and Zhang, W. (2017). Robust neural control for dynamic positioning ships with the optimum-seeking guidance. *IEEE Transactions on Systems, Man, and Cybernetics: Systems*, 47(7):1500–1509.

Zhao, D. W., Ding, F. G., Tan, J. F., Liu, Y. Q., and Bian, X. Q. (2010). Optimal thrust allocation based GA for dynamic positioning ship. In *2010 IEEE International Conference on Mechatronics and Automation, ICMA 2010*, pages 1254–1258.